Molecular Biology of the Cell
Vol. 11, 3073–3087, September 2000

Reconstitution of Brefeldin A–induced Golgi Tubulation and Fusion with the Endoplasmic Reticulum in Semi-Intact Chinese Hamster Ovary Cells[V]

Fumi Kano,*†‡ Yasushi Sako,§ Mitsuo Tagaya,‖ Toshio Yanagida,§ and Masayuki Murata†‡¶

*Department of Biophysics, Graduate School of Science, Kyoto University, Kitashirakawa, Sakyo-Ku, Kyoto 606-8502, Japan; †Department of Molecular Physiology, National Institute for Physiological Sciences, Okazaki 444-8585, Japan; ‡CREST, Japan Science and Technology Corporation, Japan; §Department of Physiology and Biosignaling, Graduate School of Medicine, Osaka University, Suita, Osaka 565-0871, Japan; and ‖School of Life Science, Tokyo University of Pharmacy and Life Science, Horinouchi, Hachioji, Tokyo 192-0392, Japan

Submitted December 23, 1999; Revised June 15, 2000; Accepted June 16, 2000
Monitoring Editor: Vivek Malhotra

The fungal metabolite brefeldin A (BFA) induces the disassembly of the Golgi complex in mammalian cells. The drug seems to accentuate tubule formation and causes the subsequent fusion with the endoplasmic reticulum (ER). To investigate the biochemical requirements and kinetics of BFA-induced Golgi disassembly, we have reconstituted the process of green fluorescent protein–tagged Golgi complex disassembly in streptolysin O–permeabilized semi-intact Chinese hamster ovary cells. For quantitative analysis of the morphological changes to the Golgi complex in semi-intact cells, we developed a novel morphometric analysis. Based on this analysis, we have dissected the BFA-induced Golgi disassembly process biochemically into two processes, Golgi tubule formation and fusion with the ER, and found that the formation is induced by only ATP and the residual factors in the cells and that the subsequent fusion is mediated in an *N*-ethylmaleimide–sensitive factor–dependent manner via Golgi tubules. Tubulation occurs by two pathways that depend on either microtubule integrity or exogenously added cytosol. In the presence of GTPγS, coat protein I inhibited the Golgi tubule fusion with the ER but showed no apparent effect on tubulation. Additionally, we analyzed the kinetics of tubulation and fusion independently in nocodazole-treated and -untreated semi-intact cells and found that tubulation is a rate-limiting step of the Golgi disassembly.

INTRODUCTION

Membrane tubular structures of the Golgi complex were found to be a ubiquitous and prominent feature of the Golgi complex that serves both to connect adjacent Golgi elements (Cluett *et al.*, 1993; Weidman *et al.*, 1993; Ladinsky *et al.*, 1994) and to carry the membrane outward along microtubules after detaching it from stable Golgi cisternae (Sciaky *et al.*, 1997; Hirschberg *et al.*, 1998).

The fungal metabolite brefeldin A (BFA), an inhibitor of Golgi vesicle formation both in vivo (Donaldson *et al.*, 1991) and in vitro (Orci *et al.*, 1991) and a membrane export out of the endoplasmic reticulum (ER) in vivo (Lippincott-Schwartz *et al.*, 1989), accentuated tubule formation but not tubule detachment (Klausner *et al.*, 1992; Lippincott-Schwartz, 1993). Sciaky *et al.* (1997) have extensively examined the dynamic properties of the Golgi complex induced by BFA in living cells with the use of the green fluorescent protein (GFP)-tagged Golgi resident protein human galactosyltransferase (GT). They found that in BFA-treated cells, many tubule networks (hereafter called Golgi tubules) formed within ~10 min of the addition of the drug and

[V] Online version of this article contains video material. Online version available at www.molbiocell. org.

¶ Corresponding author. E-mail address: mmurata@nips.ac.jp.

Abbreviations used: BFA, brefeldin A; COP I, coat protein I; GDI, GDP dissociation inhibitor; GFP, green fluorescent protein; GT, galactosyltransferase; NEM, *N*-ethylmaleimide; ROI, region of interest; SLO, streptolysin O; TB, transport buffer.

persisted for 5–10 min before rapidly fusing with the ER within 15–30 s. They proposed that because BFA augments but does not otherwise alter the morphological properties of Golgi tubules observed in BFA-untreated cells, the treatment merely accentuates a normal constitutive retrograde transport pathway between the Golgi and the ER.

With the use of the morphological dissections in living cells, the molecular mechanisms of BFA-induced Golgi disassembly are slowly beginning to be understood. Several factors have been suggested to be involved in the Golgi tubulation and the fusion. For example, calmodulin (Figueiredo and Brown, 1995) or one of its target enzymes, cytoplasmic phospholipase A_2 (Figueiredo *et al.*, 1998), is demonstrated to be involved in BFA-induced Golgi tubule formation. The microtubule-associated motor protein kinesin (Klausner *et al.*, 1992), the integrity of the microtubules, and the energy source, ATP, have been shown to be necessary for tubulation. A general fusogenic protein, *N*-ethylmaleimide–sensitive factor (NSF), is likely to be involved in the fusion process (Sciaky *et al.*, 1997; Fukunaga *et al.*, 1998). However, to our knowledge, almost all of these findings were obtained from pharmacological experiments with living cells. No direct biochemical evidence has been provided so far.

To investigate the biochemical requirements and the kinetics of Golgi tubulation and the subsequent fusion, we have reconstituted the BFA-induced Golgi disassembly process in semi-intact Chinese hamster ovary (CHO) cells. We used GFP-tagged Golgi resident membrane proteins, GFP-GT, as a probe to study Golgi morphology in intact and semi-intact cells. In this case, semi-intact cells are cells whose plasma membranes are permeabilized by the bacterial pore-forming toxin streptolysin O (SLO) (Bhakdi *et al.*, 1984). This system, coupled with GFP-tagged organelle techniques, allows one to observe the morphological effects of BFA on the Golgi complex in semi-intact cells easily and also allows biochemical manipulation while maintaining the cytoskeletal integrity of the cells. Therefore, the system is available to screen the intracellular factors involved in BFA-induced Golgi disassembly.

Using this system, we have dissected the Golgi disassembly process into two steps in semi-intact cells biochemically and morphologically: Golgi tubule formation and the subsequent fusion of Golgi tubules with ER membranes. Based on a morphometric analysis, we have developed three types of assays in semi-intact cells: a Golgi disassembly assay, a Golgi tubule formation assay, and a Golgi tubule fusion assay. Using these assays, we have found that Golgi tubule formation is induced only by both ATP and the residual factors in the semi-intact cells and that the subsequent fusion is mediated in an NSF-dependent manner via Golgi tubules. The tubules are generated by two mechanisms depending on either microtubule integrity or the exogenously added cytosol. Binding of the coat protein I (COP I) coat to the Golgi membranes inhibited the fusion of Golgi tubules and ER membranes but showed no apparent effect on tubule formation. In addition, we analyzed the kinetics of tubulation and fusion independently in nocodazole-treated semi-intact cells and found that tubulation is the rate-limiting step of the Golgi disassembly.

MATERIALS AND METHODS

Materials

Brefeldin A was purchased from Wako Pure Chemical Industries (Osaka, Japan) and used at a concentration of 10 μg/ml for intact and semi-intact cells. Nocodazole was purchased from Sigma Chemical (St. Louis, MO) and used at 2 μg/ml. Paclitaxel (taxol), 5′ adenylylimido-diphosphate (AMP-PNP), and *N*-ethylmaleimide (NEM) were obtained from Sigma Chemical. Geneticin and Lipofectamine Plus were purchased from GIBCO-BRL (Rockville, MD). The following antibodies were used: mouse anti-β-COP antibody (Sigma Chemical); mouse anti-kinesin mAb (Sigma Chemical); mouse anti-α-tubulin mAb (Sigma Chemical); mouse anti-hsp47 mAb (StressGen Biotechnologies, Victoria, British Columbia, Canada); and rabbit anti-rab6 polyclonal antibody (Santa Cruz Biotechnology, Santa Cruz, CA). SLO was purchased from Dr. Sucharit Bhakdi (University of Mainz, Germany). Bovine rab–GDP dissociation inhibitor (GDI) was donated by Dr. Hisanori Horiuchi (Kyoto University). All other chemicals were from Wako Pure Chemical Industries or NacalaiTesque (Kyoto, Japan).

Cell Culture

CHO-K1 cells were grown in Ham's F12 medium supplemented with 5% FCS, 10 mM HEPES-NaOH, pH 7.4, 100 U/ml penicillin G, 100 μg/ml streptomycin, 0.25 μg/ml fungizone, and 16 mg/ml $NaHCO_3$ at 37°C in 5% CO_2. CHO-GT (or CHO–*N*-acetylglucosaminyltransferase 1 [NAGT]), which continuously expresses GFP-GT (or GFP-NAGT), was grown with the same medium with the addition of 300 μg/ml Geneticin.

DNA Constructs and Stable Transfection

For the GFP-GT construct, cDNA encoding amino acids 1–60 of mouse GT was amplified from a mouse liver cDNA library by PCR methods. Primers were 5′-GGCCTGCAGGCATATTCCCAAAACACGA-3′ and 5′-GGCGCTAGCTTGCTTGCCTGGACCTAAGATTTTC-3′. The PCR fragment was inserted in-frame upstream of the EGFP cDNA in EGFP-N1 vector (Clontech, Palo Alto, CA). For the GFP-NAGT construct, cDNA encoding amino acids 1–103 of human NAGT was amplified from a human brain cDNA library by PCR methods and placed upstream of the EGFP cDNA in EGFP-N3 vector (Clontech). The primers for NAGT were 5′-GCCTCGAGGGATGCTGAAGAAGCAGTCTG-3′ and 5′-TCACAGGCGATGACCAGGATGGGAATCAC-3′. The PCR fragments and EGFP-N3 vectors were digested by *Xho*I–*Cfr*10I and *Xho*I–*Xba*I, respectively. The PCR fragments and vectors were ligated with DNA ligation kit version 2 (TaKaRa, Ootsu, Japan) and transformed to HB101-competent cells. CHO-K1 cells were transfected with Lipofectamine Plus (GIBCO-BRL) according to the manufacturer's instructions. Stable transfectants were selected in complete medium containing 300 μg/ml Geneticin. After 7–10 d, surviving cell colonies were isolated and screened visually for Golgi-localized fluorescence. Several positive clones were identified and expanded into cell lines for further experiments.

Preparation of Semi-Intact Cells

CHO-GT and CHO-NAGT cells were grown on a 35-mm glass-base dish (Iwaki, Funabashi, Japan) and treated with 1 ml of 60 ng/ml preactivated SLO for 10 min at 4°C. After the excess SLO had been washed away with ice-cold PBS, the cells were incubated with prewarmed transport buffer (TB; 25 mM HEPES-KOH, pH 7.4, 115 mM potassium acetate, 2.5 mM $MgCl_2$, 1 mM DTT, 2 mM EGTA) for 5 min at 32°C to form pores in the plasma membranes. The permeabilized cells were washed with ice-cold TB twice and then incubated in TB at 4°C for 20 min to elute the residual cytosol from the cells. Sixty to 70% of the total cytosol was leaked under these conditions, as determined by the measurement of cytosolic lactate

dehydrogenase leakage (Schnaar *et al.*, 1978). To ascertain the efficiency and extent of the SLO-mediated permeabilization, we tested the accessibility of intracellular actin to exogenously added rhodamine-labeled phalloidin, a small bicyclic peptide that binds with high affinity to F-actin filaments (Barak *et al.*, 1980). No staining of actin with rhodamine–phalloidin was observed in intact CHO-GT cells, but the semi-intact cells prepared by SLO treatment exhibited staining of actin filaments, demonstrating that the semi-intact cells allowed access to small molecules such as rhodamine–phalloidin (1.2 kDa). Under the same conditions, staining of microtubules with anti-α-tubulin antibody (immunoglobulin G) was also observed in semi-intact cells. Although >99% of the cells on the glass-base dish were found to be permeabilized by this SLO treatment, the intensity of the staining varied among cells, suggesting that some cells had more or larger holes than others. However, the variations in the efficiency and extent of permeabilization were too small to affect the quantitative assays by morphometric analysis described below; almost all data showed very small SDs, i.e. <10%.

Immunofluorescence and Time-lapse Microscopy

In the case of double staining with the use of the anti-hsp47, β-COP, α-tubulin, and GM-130 monoclonal and polyclonal antibodies, the cells were permeabilized and fixed with methanol:acetone (1:1, vol/vol) at 0°C for 6.5 min and then incubated with TB containing 5% skim milk for blocking. The cells were incubated with primary antibodies in TB containing 5% skim milk for 2 h, washed to remove free antibody, and then incubated with the fluorescently labeled secondary antibodies for 1 h at room temperature. After being washed, glass-base dishes were directly viewed with a 63× Planapo lens on an Axiovert 135 fluorescence microscope (Carl Zeiss, Jena, Germany) equipped with a color-chilled charge-coupled device camera (model C5810-01, Hamamatsu Photonics, Hamamatsu, Japan). Time-lapse images of Golgi membranes were viewed with a confocal microscope (LSM510, Carl Zeiss).

Morphometric Analysis

Semi-intact CHO-GT cells were incubated under various conditions and then fixed with 1% formaldehyde in TB at room temperature for 20 min. The fixed specimens were viewed with the fluorescence microscope described above. For morphometric analysis, we enumerated the cells in which the Golgi complex was intact, referred to as "intact Golgi"; the cells in which BFA-induced Golgi tubules were observed, referred to as "tubular Golgi" (this stage was defined by Golgi connecting with tubular structures and being more than 5 μm long); and the cells in which the Golgi membranes fused with the ER membranes, referred to as " fused Golgi." Because the Golgi apparatus sometimes appeared to be fragmented, multiple fusion events might be required for complete Golgi disassembly to the ER. Some of the tubules that extended from the separated Golgi elements fused with the ER, whereas others remained intact. In these cases, we counted such cells as "tubular Golgi." On triplicate coverslips, cells were counted in three hundreds in random fields in each sample, and morphometric analysis was performed. Morphological changes to Golgi complexes were expressed as the percentages of cells having intact Golgi, tubular Golgi, or fused Golgi in each sample. Three independent experiments were performed, and means and SDs were calculated.

Golgi Disassembly Assay

This assay was used to study the whole process of BFA-induced Golgi disassembly in semi-intact cells. Semi-intact CHO-GT cells were incubated under various conditions with an ATP-regenerating system (1 mM ATP, 8 mM creatine kinase, and 50 μg/ml creatine phosphate), 1 mg/ml glucose, 1 μg/ml rhodamine–phalloidin, 10 μg/ml BFA, and L5178Y cytosol (1.7–2.5 mg/ml protein concentrations) at 32°C for various times. After the incubation, cells were fixed with 1% formaldehyde in TB at room temperature for 20 min and then subjected to morphometric analysis.

Golgi Tubule Formation Assay

This assay was used to study BFA-induced Golgi tubule formation. At first, semi-intact CHO-GT cells were incubated, under various conditions or in the presence of the reagents to be tested, with the ATP-regenerating system and 10 μg/ml BFA in TB at 32°C for 80 min. Alternatively, in several experiments, semi-intact cells were incubated with the ATP-regenerating system, BFA, and NEM-treated L5178Y cytosol. After the incubation, cells were fixed and subjected to morphometric analysis. In some cases, after incubation, cells were washed extensively with TB at 0°C for 20 min and then further incubated under various conditions and used for the Golgi tubule fusion assay.

Golgi Tubule Fusion Assay

This assay was used to study the fusion between the BFA-induced Golgi tubules and ER membranes. At first, Golgi tubule formation was induced as described in Golgi Tubule Formation Assay, and then the cells were washed extensively with TB at 0°C for at least 20 min. After being washed, the cells were further incubated, under various conditions or in the presence of the reagents to be tested, with the ATP-regenerating system and were subjected to morphometric analysis. BFA in the incubation mixtures did not affect the efficiency of Golgi tubule fusion.

Cytosol Preparation

L5178Y cytosol was prepared by the method used to prepare HeLa cytosol (Pimplikar *et al.*, 1994). All procedures were performed at 0°C to obtain cytosol containing the active NSF. Protein concentrations were determined with BSA as a standard with the use of the Bio-Rad (Richmond, CA) protein assay. Rat cytosol was prepared by the method described by Sakaguchi *et al.* (1992).

Nocodazole Treatment of Intact Cells and rab-GDI Treatment of Semi-Intact Cells

CHO-GT cells grown on the coverslips or the glass-base dish were placed on ice for 20 min and then for 30 min in the presence of 2 μg/ml nocodazole and subsequently incubated at 37°C for 20 min. The depolymerization of microtubules in the cells was detected by an indirect immunofluorescence method for fixed specimens or by direct observation with the use of CHO cells expressing GFP–α-tubulin. Semi-intact CHO cells were treated with rab-GDI by the method described by Ullrich *et al.* (1995).

NEM Treatment of the Cytosol

L5178Y cytosol (1.7–2.4 mg/ml protein concentration) was treated with 2 mM NEM at 0°C for 60 min and then quenched with 8 mM DTT at 0°C for 60 min. The mock NEM–cytosol was prepared by mixing both NEM and DTT at the beginning of the incubation.

Kinetic Modeling of Golgi Disassembly

To extract the kinetic information on BFA-induced Golgi disassembly in semi-intact cells, we used a model (a simple linear first-order kinetics model), shown in Figure 10, that contained two rate constants: k_1, the Golgi tubule formation rate, and k_2, the Golgi tubule fusion rate. Two or three data sets for the percentage of cells having intact Golgi, tubular Golgi, or fused Golgi were fitted simultaneously with the use of the generalized least-squares optimization procedure in the Sigmaplot scientific graph system, version 4.11 (Jandel, CA), to quantify the rate constants. To obtain the optimal fitting for the curves of Golgi tubule formation or Golgi tubule fusion, we subtracted the percentage of intact Golgi or tubular Golgi

from the total (100%) because they seem to be experimental deviations of the Golgi tubule formation assay or the Golgi tubule fusion assay, respectively.

RESULTS

Reconstitution of BFA-induced Golgi Disassembly in Semi-Intact Cells

To investigate the dynamic properties of the Golgi membranes treated with BFA in semi-intact CHO cells, we used GFP-GT and GFP-NAGT as fluorescence probes, both of which have been used in the study of Golgi membrane dynamics in living cells (Cole *et al.*, 1996b; Sciaky *et al.*, 1997; Shima *et al.*, 1997). The stable transfectant, CHO-GT, was incubated with 10 μg/ml BFA at 30°C and viewed with a confocal microscope equipped with a time-lapse image-capture system. In BFA-treated cells, long and motile Golgi tubules containing GFP-GT were generated and persisted for 3–10 min, and tubule formation was followed by the rapid fusion of Golgi and ER membranes within 1 min (Figure 1A, intact; online version of Figure 1A, intact, is available at www.molbiolcell.org). The cells in a state of postfusion show a characteristic diffuse staining pattern of the ER networks through the cytoplasm and are easily distinguishable from other cells morphologically (compare intact Golgi with fused Golgi in Figure 1A). To ascertain that the diffusive staining pattern shows the ER networks, we confirmed the localization of GFP-GT of fused Golgi and hsp47, whose epitope is mainly localized in the ER, by an indirect immunofluorescence method with the use of anti-hsp47 antibody. We observed almost the same effects of BFA on the dynamics of the GFP-tagged Golgi complex in another stable transfectant, CHO-NAGT.

Next, we reconstituted the process of BFA-induced Golgi disassembly in semi-intact CHO-GT cells. At first, semi-intact CHO-GT cells were incubated in the presence of 10 μg/ml BFA, cytosol (protein concentration of 2.5 mg/ml), and the ATP-regenerating system (hereafter referred to as ATP) at 30°C and viewed with a confocal microscope. BFA-induced Golgi tubule formation followed by the fusion was observed as in intact CHO-GT cells (Figure 1A, semi-intact; online version of Figure 1A, semi-intact, is available at www.molbiolcell.org).

The disassembly of the Golgi complex in intact and semi-intact cells was also monitored quantitatively by following the changes in fluorescence intensities (averaging fluorescence intensity/area) of the regions of interest (ROIs) corresponding to the Golgi region and the cytoplasmic ER network (Figure 1B). Upon disassembly of the complex, the fluorescence intensities of GFP-GT associating with the Golgi elements or Golgi tubules (ROI 1) suddenly decreased; in contrast, those of ER networks (ROIs 2–4) correspondingly increased. As a result, both fluorescence intensities reached a similar level. In semi-intact cells, a similar change in fluorescence intensity was observed upon BFA treatment, but the decrease of intensity in the Golgi region was more moderate than that in intact cells (Figure 1B, b).

Dissection of the Process of BFA-induced Golgi Disassembly in Semi-Intact Cells

We could dissect the process of BFA-induced Golgi disassembly biochemically in semi-intact cells. Semi-intact cells were incubated with 10 μg/ml BFA in TB at 30°C for 80–240 min. The Golgi complex, which was visualized with GFP-tagged proteins, remained almost intact even after 240 min of incubation. This suggested that the cytosolic factors, an energy source such as ATP, or both were necessary for BFA-induced Golgi disassembly. Next, semi-intact cells were incubated with BFA/cytosol, BFA/ATP, or BFA/cytosol/ATP at 30°C for 80 min. As expected, the Golgi was disassembled in the presence of both cytosol and ATP (Figure 2c). In contrast, in the absence of ATP, the Golgi complex remained intact even in the presence of cytosol (Figure 2a). Interestingly, even in the absence of exogenously added cytosol, BFA-induced Golgi tubule formation was observed very often in the presence of ATP but fusion was not (Figure 2b).

We could dissect the disassembly process biochemically in a single semi-intact cell. At first, semi-intact CHO-GT cells were incubated with 10 μg/ml BFA and ATP (without cytosol) in TB at 30°C and were imaged at 5-min intervals with the use of a fluorescence microscope. Figure 3 shows a typical Golgi tubule formation in semi-intact CHO-GT cells in the presence of BFA and ATP. In our reconstitution system, tubule formation was usually initiated at 10–20 min after the addition of BFA and persisted for 20–240 (or more) minutes. Although in overall appearance and properties, the Golgi tubules in semi-intact cells were similar to those in intact cells, they did not fuse with the ER and extended enormous lengths (up to 60 μm) with long and winding shapes.

At the second step, after being washed with cold TB, the semi-intact cells were further incubated with BFA/cytosol/ATP at 30°C. The motility and efficiency of bifurcation of Golgi tubules increased, but the average length and number of tubules did not. At ~20–30 min after the addition of BFA/cytosol/ATP (2.5 mg/ml protein concentration), several Golgi tubules and their connected Golgi elements disappeared suddenly over a period of ~5 min. At the same time, the corresponding area of the cytoplasmic ER networks grew brighter (Figure 3, lower panels).

Based on the morphological changes of Golgi membranes, we dissected the BFA-induced Golgi disassembly into two processes in the semi-intact cells. In the first process, the tubules were generated without detachment from the Golgi elements. Their formation requires the energy source ATP exogenously. In the second process, the extended Golgi tubules fused with the ER networks. This process is dependent on both ATP and cytosol. However, we cannot rule out the possibility that the residual factors in the semi-intact cells were involved in tubulation and that Golgi elements fuse directly with the ER membranes. We obtained similar results for the BFA-treated semi-intact CHO-NAGT cells. Thereafter, we used semi-intact CHO-GT cells for subsequent experiments.

Morphometric Analysis of the Golgi Tubulation Process

Because semi-intact cells were virtually indistinguishable from intact cells with regard to the relocation of Golgi resident membrane proteins to the ER in BFA-treated cells, we developed a novel morphometric analysis (see MATERIALS AND METHODS) to quantify the morphological changes of the Golgi complex in semi-intact cells.

At first, morphometric analysis was applied to investigate the biochemical requirements of Golgi tubule formation. Semi-intact cells were incubated with 10 μg/ml BFA under

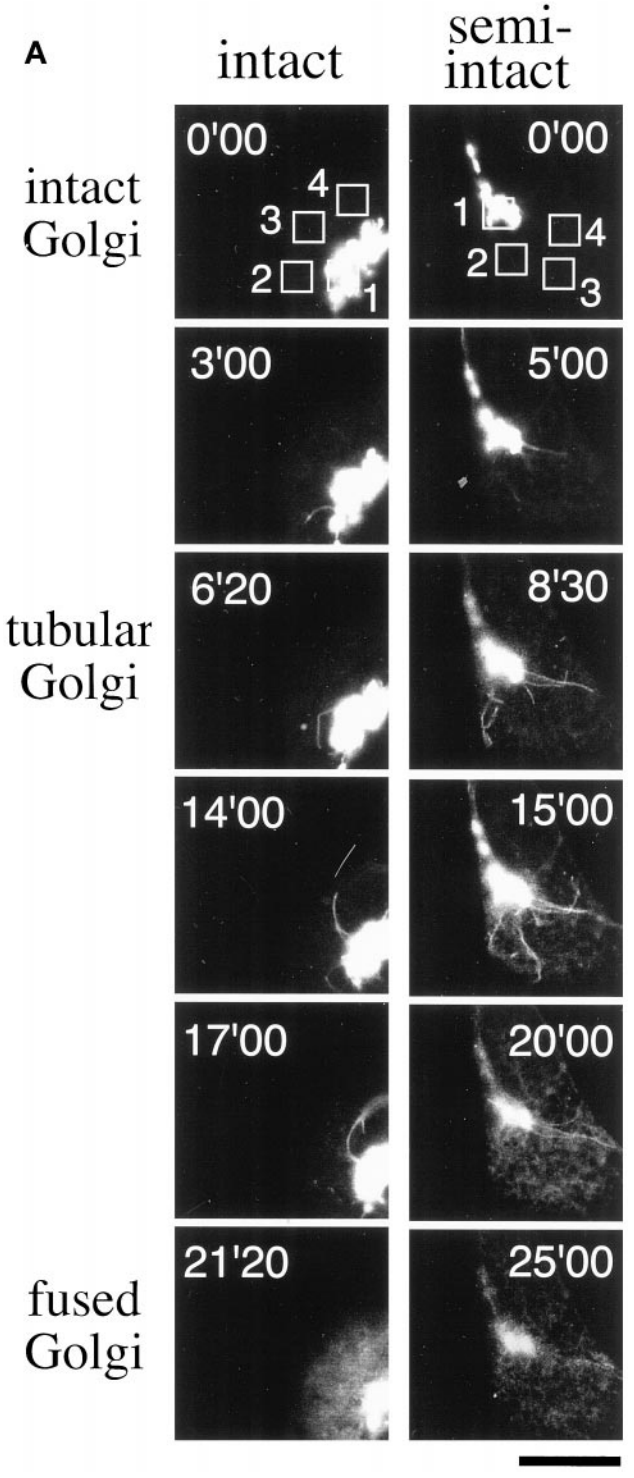

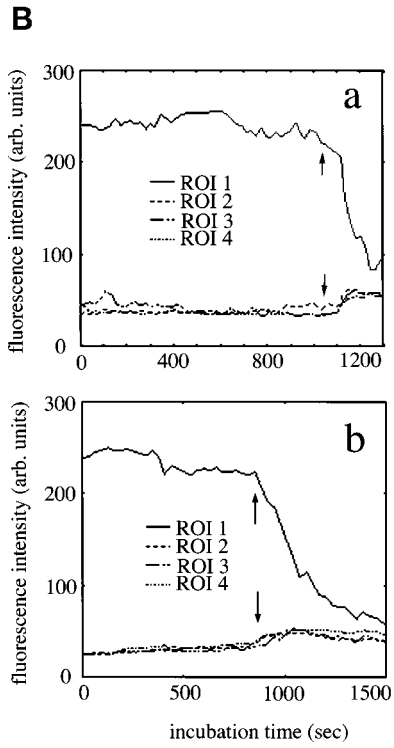

Figure 1. The formation and subsequent fusion to the ER networks of Golgi tubules in intact and semi-intact CHO-GT cells. (A) Intact CHO-GT cells incubated with 10 μg/ml BFA were imaged at 5-s intervals with the use of a confocal microscope equipped with a time-lapse image-acquisition system at 30°C. Semi-intact CHO-GT cells incubated with 10 μg/ml BFA in the presence of cytosol and ATP were imaged as described in the text. The cells having intact Golgi, tubular Golgi, and fused Golgi are shown. Incubation times are indicated in each panel. Bar, 10 μm. (B) Fluorescence intensities associated with the Golgi ROI (ROI 1) and cytoplasm ROIs (ROIs 2–4) in the intact (a) and semi-intact (b) cells in Figure 1A are plotted at 5-s intervals for 20 or 25 min. Arrows indicate the approximate times of Golgi disassembly. There are corresponding increases in the fluorescence intensities of cytoplasm ROIs.

various conditions for 80 min and fixed, and then the Golgi tubule formation assay was conducted. We fixed the incubation conditions (32°C for 80 min) and compared the data obtained from the assays in the subsequent experiments.

Golgi tubule formation required ATP and was dependent on ATP hydrolysis (Figure 4, ATP and AMP-PNP). The nonhydrolyzable GTP analogue GTPγS (Figure 4, GTPγS) or the general kinase inhibitor staurosporin had no effect on

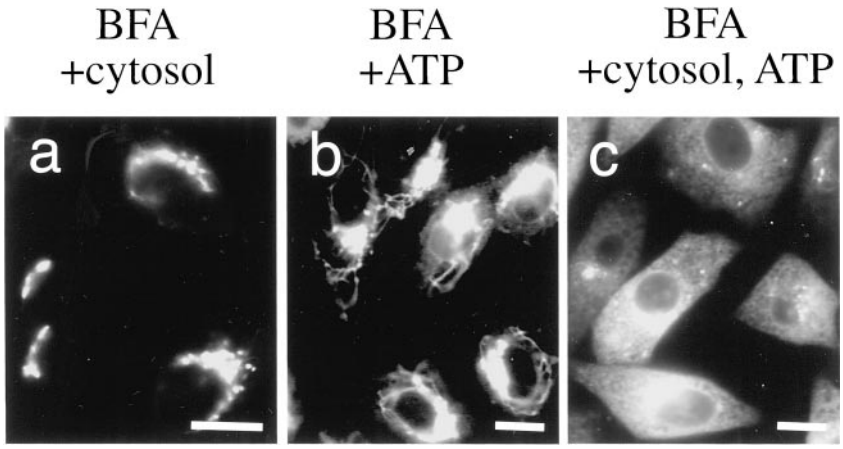

Figure 2. Cytosol and ATP requirements for BFA-induced Golgi disassembly. Semi-intact cells were incubated with BFA/cytosol, BFA/ATP, or BFA/cytosol/ATP at 30°C for 60 min and then fixed. The samples were viewed with the use of a fluorescence microscope. Bars, 10 μm.

tubulation. Interestingly, in the presence of cytosol (2.5 mg/ml), tubulation was completely inhibited by GTPγS. A high-salt wash, which resulted in the release of the peripheral membrane proteins, partially inhibited tubulation (Figure 4, KCl). We investigated the effect of a commercial mAb against kinesin on tubulation. However, coincubation with 10–100 μg/ml antibodies did not affect tubulation, although the antibody was confirmed to have penetrated the semi-intact cells by an indirect immunofluorescence method. Next, we examined the involvement of another Golgi-related motor protein, rabkinesin-6, in tubulation. Rabkinesin-6 has been reported to bind to the GTP form of rab6 and function as a motor (Echard *et al.*, 1998). We treated the semi-intact cells with rab-GDI to deplete rab6. We confirmed

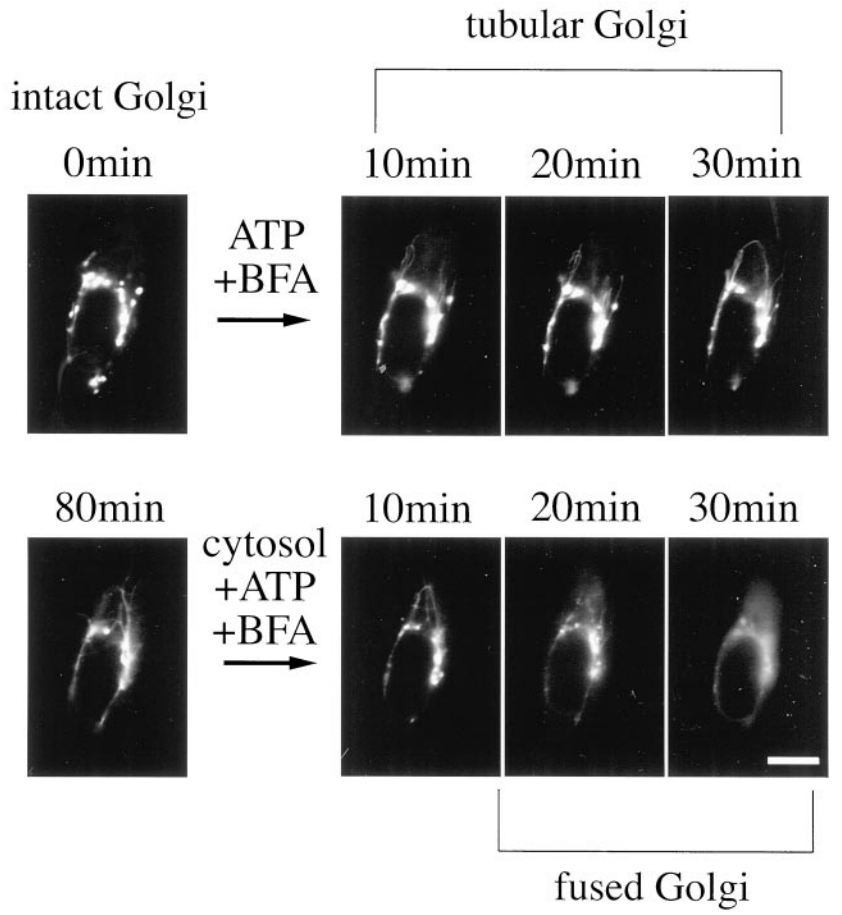

Figure 3. Morphological dissection of the BFA-induced Golgi disassembly process in a single semi-intact cell. Semi-intact cells were incubated with BFA/ATP at 30°C for 80 min to generate the Golgi tubules. After being washed, the cells were further incubated with BFA/cytosol/ATP for 80 min. The sample was imaged at 5-min intervals with the use of a conventional fluorescence microscope. The Golgi tubules fused with the ER networks only in the presence of both exogenous cytosol and ATP. Bar, 10 μm.

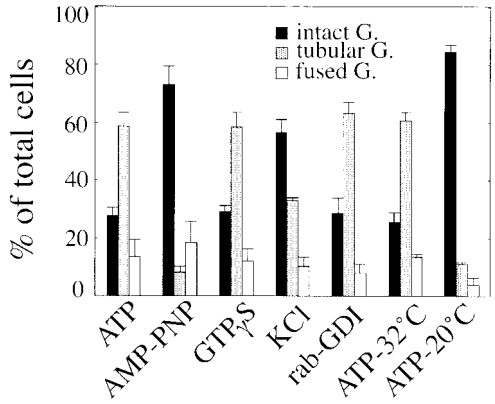

Figure 4. Biochemical requirements for BFA-induced Golgi tubule formation in semi-intact cells. Semi-intact CHO-GT cells were incubated with BFA and an ATP-regenerating system (ATP), 1 mM AMP-PNP (AMP-PNP), or 0.2 mM GTPγS/ATP (GTPγS) at 32°C for 80 min. Semi-intact cells were treated with 1.0 M KCl at 0°C for 30 min (KCl) or 0.8 μM rab-GDI at 33°C for 30 min (rab-GDI) and then incubated with BFA/ATP at 32°C for 80 min. Other cells were incubated with BFA/ATP at 32°C or at 20°C for 80 min (ATP-32°C, ATP-20°C). At least 300 cells were counted for each sample. Cells were counted in three randomly selected fields. Three independent experiments were performed, and means and SDs were calculated.

the depletion by Western blotting with the use of anti-rab6 antibody. More than 95% of the protein was depleted from the semi-intact cells. However, the treatment had no effect on tubulation (Figure 4, rab-GDI). Golgi tubule formation was also dependent on the incubation temperature. Tubulation was completely inhibited at temperatures < 20°C (Figure 4, ATP-32°C and ATP-20°C).

The ATP-driven motor proteins or other peripheral proteins, which cycle between the cytosol and peripheral association with Golgi membranes, might be involved in Golgi tubule formation, but exogenously added cytosol was not always essential for tubulation.

Effects of Exogenous Cytosol on BFA-induced Golgi Tubule Formation

We investigated more closely the exogenous cytosol requirement of Golgi tubule formation in semi-intact cells. From another experiment, we had already found that NEM-treated cytosol (hereafter called NEM cytosol) induced Golgi tubule formation but did not induce fusion, probably because NSF was inactivated.

In the presence of NEM cytosol, the generated tubules were slightly shorter; the average length was 15 ± 3.8 μm (n = 100) and 10 ± 2.2 μm (n = 100) in the absence and presence of NEM cytosol, respectively. However, morphometric analysis suggested that the efficiency of Golgi tubule formation was almost the same: 52.0 ± 1.7% and 59.6 ± 7.9%. In addition, the number of Golgi tubules (>20 μm) per cell was 2.2 ± 0.2 and 1.8 ± 0.1 in the absence and presence of NEM cytosol, respectively. We also found that further addition of NEM cytosol affected neither the numbers nor the lengths of preformed Golgi tubules. However, the addition of NEM cytosol vigorously facilitated the motility and

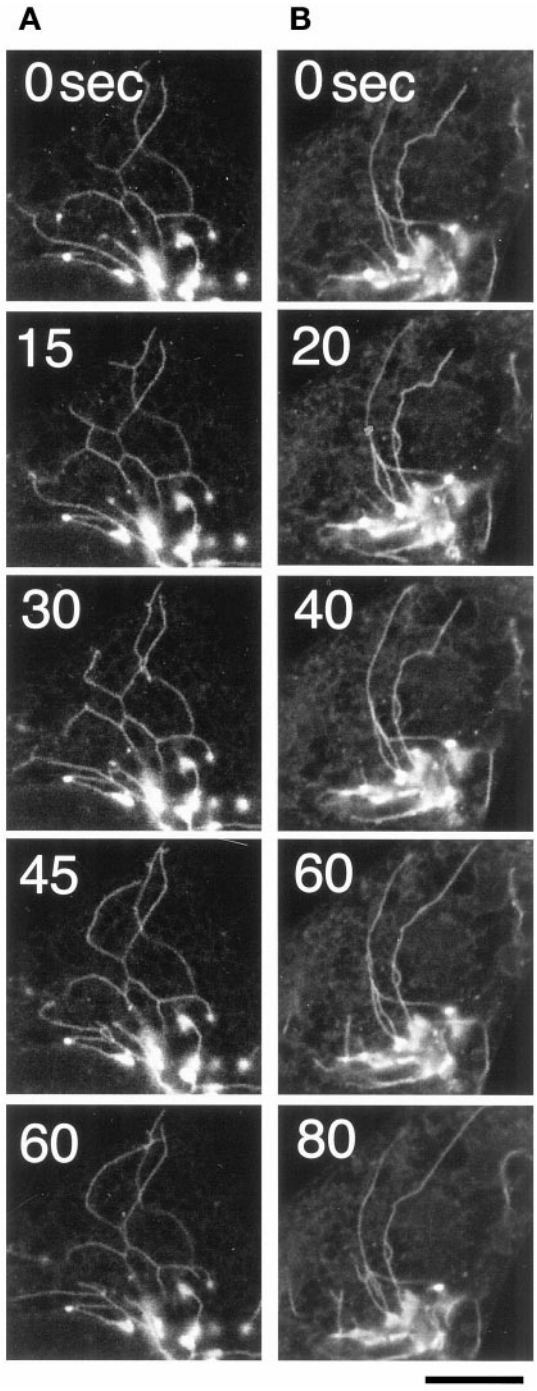

Figure 5. Effects of cytosol on BFA-induced Golgi tubule formation in semi-intact cells. Golgi tubule formation was observed in the presence of NEM cytosol/BFA/ATP (A) or BFA/ATP (B) in semi-intact CHO-GT cells. In both cases, the efficiency of the formation was almost the same. However, the motility of the tubules and the frequency of their bifurcation appeared to be increased slightly in the presence of NEM cytosol. Bar, 10 μm.

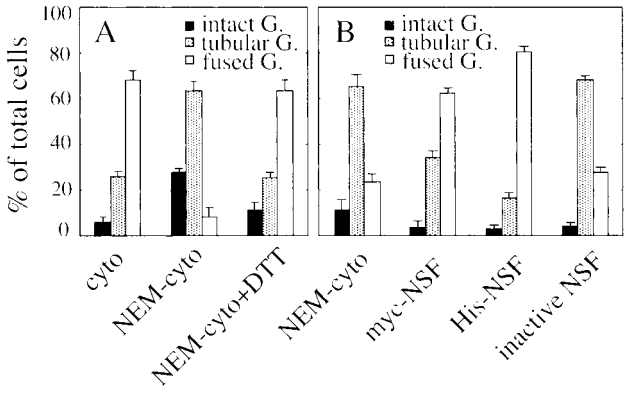

Figure 6. Biochemical requirements for BFA-induced Golgi disassembly (A) and Golgi tubule fusion (B) in semi-intact cells. (A) Semi-intact CHO-GT cells were incubated with either BFA/ATP/cytosol (cyto), BFA/ATP/NEM-treated cytosol (NEM-cyto), or BFA/ATP/NEM-treated cytosol/DTT (NEM-cyto+DTT) at 32°C for 80 min, fixed, and then subjected to morphometric analysis (Golgi disassembly assay). The protein concentration of the cytosol used in this experiment was 1.7 mg/ml. (B) At first, semi-intact cells were incubated with BFA/ATP at 32°C for 80 min to generate the Golgi tubules. About 65% of cells had Golgi tubules. Then the cells were further incubated with BFA/ATP/NEM-treated cytosol (NEM-cyto), BFA/ATP/NEM-treated cytosol/myc-NSF (myc-NSF), BFA/ATP/NEM-treated cytosol/His-NSF (His-NSF), or BFA/ATP/NEM–treated cytosol/K266Q-NSF (inactive NSF) at 32°C for 80 min, and morphometric analysis was performed (Golgi tubule fusion assay). The protein concentration of the cytosol used was 2.3 mg/ml. Three hundred cells were counted for each sample. Cells were counted in three randomly selected fields. Three independent experiments were performed, and means and SDs were calculated.

bifurcation of the preformed Golgi tubules (Figure 5, A and B; online version of Figure 5 is available at www.molbiolcell.org).

The double-staining experiments revealed that, in both cases, the generated Golgi tubules did not always associate along microtubules. Some of them extended independently of microtubules.

Morphometric Analysis of the Golgi Tubule Fusion Process

The second process in BFA-induced Golgi disassembly is the fusion of the Golgi and ER membranes. The fusion event seems to be mediated by a general fusogenic protein, NSF, via BFA-induced Golgi tubules (Sciaky *et al.*, 1997; Fukunaga *et al.*, 1998). To prove this, we prepared and tested three types of cytosol: NEM-treated cytosol (NEM cytosol), cytosol treated with NEM and DTT simultaneously as a mock cytosol (NEM cytosol/DTT), and untreated cytosol (cytosol). In the presence of either NEM cytosol/DTT or cytosol, fusion occurred in semi-intact cells. In contrast, in the presence of NEM cytosol, fusion was completely inhibited but Golgi tubule formation was not (Figure 6A). This strongly indicates that NSF might be involved in the fusion process but not in Golgi tubule formation in our semi-intact cells.

To further ascertain that this loss of fusion activity in NEM cytosol is due to NSF inactivation, several recombinant NSFs were prepared (Sumida *et al.*, 1994; Fukunaga *et al.*, 1998) and used to rescue the fusion activity of NEM cytosol. For the assay, semi-intact cells were preincubated with NEM cytosol in the presence of ATP and BFA to induce Golgi tubule formation. By this treatment, ~65% of cells were sustained in the stage showing tubular Golgi (Figure 6B, NEM cytosol). The cells having the tubular Golgi were subsequently incubated with ATP/BFA and NEM cytosol, NEM cytosol containing recombinant myc-NSF (40 μg/ml), NEM cytosol containing recombinant His-NSF (40 μg/ml), or NEM cytosol containing recombinant inactive mutant NSF (K266Q) (40 μg/ml). As shown in Figure 6B, addition of the first two recombinant NSFs restored fusion activity, from 25 to 65% for myc-NSF and to 80% for His-NSF. In contrast, the addition of inactive mutant NSF (K266Q) had no effect on fusion efficiency. This loss of fusion activity upon NEM treatment and its restoration with the addition of recombinant NSFs is a convincing demonstration of the essential role of NSF in the fusion between Golgi tubules (Golgi elements) and ER membranes.

Inhibitory Effect of Coat Proteins on Golgi Tubule Fusion

To investigate the regulatory role of the coat protein, COP I coat, in Golgi tubulation or in fusion of the Golgi tubules and ER membranes, we investigated the effects of GTPγS or β-COP on tubulation or fusion. For these experiments, we used the rat cytosol instead of L5178Y cytosol because our antibody against β-COP did not work for an immunodepletion experiment to the L5178Y cytosol. The rat cytosol (mock; 2.5 mg/ml) was indistinguishable from L5178Y cytosol with regard to Golgi disassembly, Golgi tubule formation, and Golgi tubule fusion.

Although incubation of the semi-intact cells with 0.4 mM GTPγS/ATP/BFA induced tubulation, incubation with 0.4 mM GTPγS/ATP/BFA/NEM-treated rat cytosol (mock) completely inhibited it (Figure 7A, mock). Next, we prepared the β-COP–depleted rat cytosol [cyto ($-\beta$-COP)]. The depletion of β-COP was confirmed by Western blotting (Figure 7C). GTPγS/ATP/BFA/NEM-treated cytosol ($-\beta$-COP) also showed the inhibitory effect on tubulation [Figure 7A, cyto ($-\beta$-COP)]. Indirect immunofluorescence experiments revealed a faint staining of β-COP on the Golgi elements in all cases described above. However, such a small amount of β-COP did not inhibit the BFA-induced, ATP-driven Golgi tubulation in the presence of GTPγS (Figure 4). These results indicate that a GTPγS-sensitive cytosolic factor other than COP I coat might be involved in BFA-induced Golgi tubule formation (see DISCUSSION).

Next, the semi-intact cells having BFA-induced Golgi tubules were incubated with 0.4 mM GTPγS/ATP/BFA/cytosol (mock), and then the Golgi tubule fusion assay was performed. The fusion of Golgi tubules to the ER membranes was inhibited (Figure 7B, mock). In contrast, incubation with 0.4 mM GTPγS/ATP/BFA/cytosol ($-\beta$-COP) induced fusion [Figure 7B, cyto ($-\beta$-COP)]. This indicates that COP I coat inhibited the fusion between the Golgi tubules and the ER membranes. Indirect immunofluorescence experiments revealed a substantial association of β-COP on the preformed Golgi tubules or Golgi elements even in the presence of BFA when fusion was inhibited (Figure 7D). In the

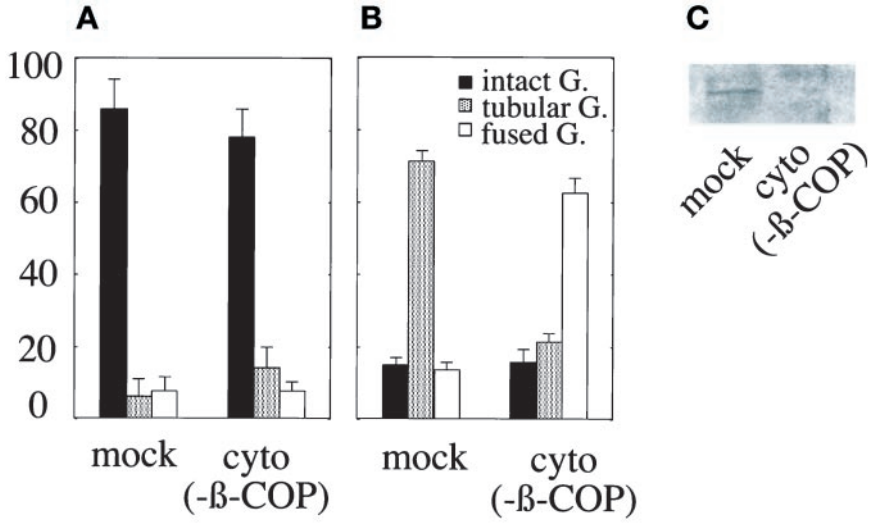

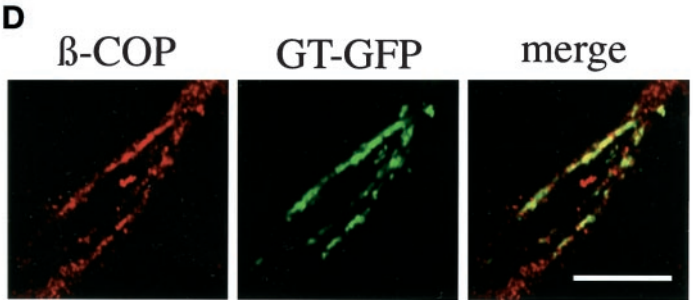

Figure 7. Effect of β-COP depletion on Golgi tubule formation and fusion. Either mock [mock]- or β-COP–depleted [cyto (−β-COP)] rat cytosol containing GTPγS and ATP-regenerating system were subjected to the Golgi tubule formation assay (A) or the Golgi tubule fusion assay (B). The extent of β-COP depletion was determined by immunoblotting (C). When the semi-intact cells were incubated with mock cytosol, GTPγS, and ATP in the Golgi tubule fusion assay, β-COP was found to associate with preformed Golgi tubules as shown in D. Bar, 10 μm.

case of cytosol (−β-COP), no substantial association of β-COP was observed.

BFA-induced Golgi Disassembly in the Microtubule Disrupted Semi-Intact Cells

To investigate the effect of microtubules on Golgi disassembly, our reconstitution analysis was applied in nocodazole-treated semi-intact CHO-GT cells. First we treated the CHO-GT cells with nocodazole (2 μg/ml) as described in MATERIALS AND METHODS to depolymerize microtubules (Cole *et al.*, 1996a). After washing the cells, we prepared semi-intact cells by a two-step procedure of SLO. The treatments of nocodazole and SLO did not affect the Golgi morphology significantly, although there appeared to be less clustering. Almost all fluorescence localized within the Golgi structure. Microtubule disruption was checked after the experiments by an indirect immunofluorescence method (Figure 8B) and visualized directly with the use of GFP–α-tubulin–transfected CHO cells. Almost all of the microtubule networks were destroyed by the nocodazole treatment, although they partially remained, especially around the cell periphery (Figure 8B).

The semi-intact cells were incubated with either BFA/ATP or BFA/ATP/cytosol at 32°C for 80 min. As expected from the result with nocodazole-treated intact cells (Sciaky *et al.*, 1997), Golgi tubule formation was completely inhibited (Figure 8A, ATP), although fusion was not affected (Figure 8A, cytosol). Surprisingly, when the semi-intact cells were incubated with NEM cytosol in the presence of BFA/ATP, the formation proceeded normally (Figure 8A, NEM-cyto). We ascertained by immunofluorescence methods that incubation with NEM cytosol did not cause microtubule reformation at the fluorescence microscopic level (Figure 8B). The distribution of the lengths of BFA-induced Golgi tubules was also analyzed and found to be very similar to that in nocodazole-untreated cells; the average length was 15 ± 3.5 μm (n = 100). When the NEM cytosol–treated cells were further incubated with NEM cytosol containing His-NSF (40 μg/ml), the Golgi tubules fused with the ER (Figure 8A, NEM-cyto+His-NSF).

These results strongly indicate that, even in microtubule-disrupted semi-intact cells, BFA-induced Golgi disassembly may involve two processes, Golgi tubule formation and subsequent NSF-dependent fusion with the ER. However, microtubule disruption affects the initial stage of BFA-induced Golgi tubulation. The newly added NEM cytosol restored tubule formation. This, together with the results shown in Figures 4 and 8B, indicates that Golgi

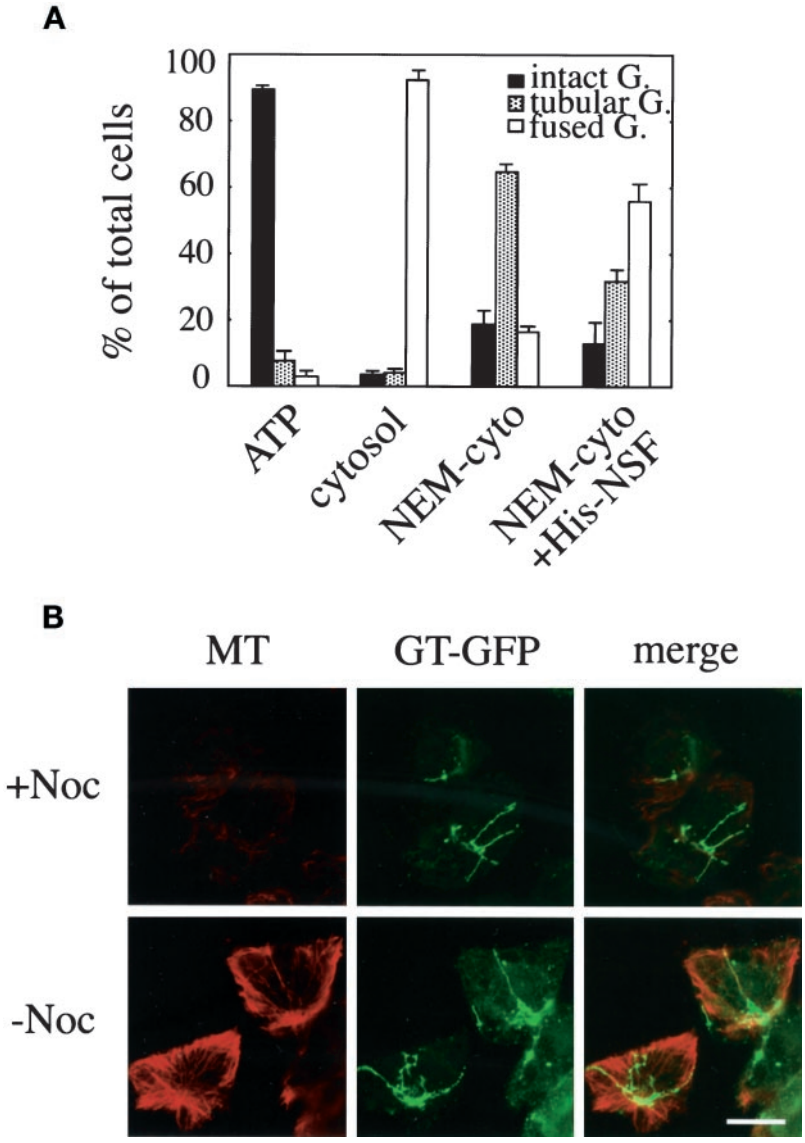

Figure 8. Biochemical requirements for BFA-induced Golgi disassembly in microtubule-disrupted semi-intact cells. (A) CHO-GT cells were treated with nocodazole to depolymerize microtubules and then permeabilized by SLO. The drug-treated semi-intact cells were incubated with BFA/ATP (ATP), BFA/ATP/cytosol (cytosol), or BFA/ATP/NEM-treated cytosol (NEM-cyto) at 32°C for 80 min, fixed, and then subjected to morphometric analysis (Golgi disassembly assay). The drug-treated semi-intact cells incubated with BFA/ATP/NEM-treated cytosol at 32°C for 80 min were washed and then further incubated with BFA/ATP/NEM-treated cytosol/His-NSF at 32°C for 60 min. Again, morphometric analysis was performed (NEM-cyto+His-NSF). The protein concentration of the cytosol used was 2.5 mg/ml. At least 300 cells were counted for each sample. Cells were counted in three randomly selected fields. Three independent experiments were performed, and means and SDs were calculated. (B) Golgi tubules in the presence or absence of nocodazole treatment. Nocodazole-treated (+Noc) or -untreated (−Noc) semi-intact cells were incubated with BFA/ATP/NEM-treated cytosol at 32°C for 80 min. Then, microtubules (MT) were visualized by the immunofluorescence method with the use of anti-α-tubulin antibody. Bar, 10 μm.

tubule formation is induced by two pathways depending on either microtubule integrity or exogenously added cytosol.

Kinetic Analysis of BFA-induced Golgi Disassembly in Semi-Intact Cells: Effects of Microtubule Disruption

Based on the biochemical requirements described above, we used our three assays to study the kinetics of the BFA-induced Golgi disassembly process in nocodazole-treated or -untreated semi-intact CHO-GT cells. To investigate the effects of microtubule disruption on the kinetics of BFA-induced Golgi disassembly (the entire process), we performed the Golgi disassembly assay for nocodazole-treated semi-intact CHO-GT cells, which were prepared as described above. Figure 9 (compare A and E) reveals that microtubule disruption markedly affected the disassembly rates. Although the maximum half-time of disassembly was ~12 min for untreated cells, that for treated cells increased to >40 min.

Next, to determine which process, Golgi tubule formation or Golgi tubule fusion, affects the disassembly rate in nocodazole-treated semi-intact cells, we performed the formation assay and fusion assay independently for each sample and compared their kinetics. In the Golgi tubule formation assay, we used NEM cytosol to induce formation and compared the rates of formation. As shown in Figure 9, B and F, the rate of Golgi tubulation was markedly affected by nocodazole treatment, but the rate of fusion was not (Figure 9, C and G). These results suggest that the rate-limiting step of BFA-induced Golgi disassembly in microtubule-disrupted semi-intact cells is the Golgi tubule formation process.

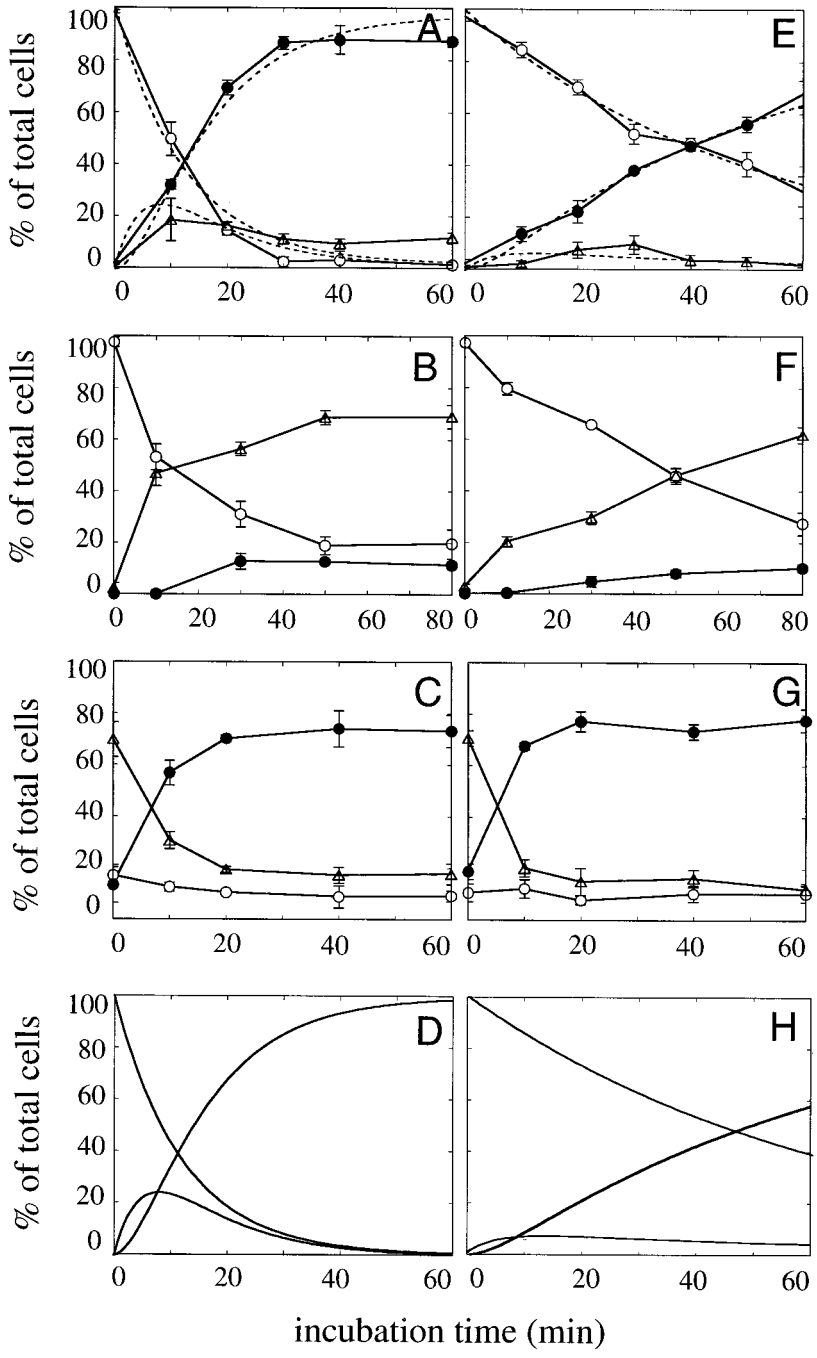

Figure 9. Kinetics of each process of BFA-induced Golgi disassembly in nocodazole-untreated (A–D) and -treated (E–H) semi-intact CHO-GT cells. Intact CHO-GT cells were treated with nocodazole (2 μg/ml) as described in the text to depolymerize microtubules and then permeabilized by SLO. (A and E) Drug-untreated or -treated semi-intact cells were incubated with BFA/ATP/cytosol at 32°C for various periods, fixed, and then subjected to morphometric analysis (Golgi disassembly assay). Dotted lines indicate the simulation curves, which were simultaneously fitted to the data plots according to the successive reaction model shown in Figure 10. (B and F) The cells were incubated with BFA/ATP/NEM-treated cytosol at 32°C for various periods and then analyzed as described above (Golgi tubule formation assay). (C and G) The cells were incubated with BFA/ATP/NEM-treated cytosol at 32°C for 60 min to generate the Golgi tubules. After being washed, the cells were further incubated with BFA/ATP/cytosol at 32°C for various periods, fixed, and subjected to morphometric analysis (Golgi tubule fusion assay). The protein concentration of the cytosol used was 2.3 mg/ml. Three hundred cells were counted in three randomly selected fields for each time point. Three independent experiments were performed, and means and SDs were calculated. (D and H) Simulated curves for the Golgi disassembly process. With the use of the rate constants obtained from the Golgi tubule formation assay (B and F) and the Golgi tubule fusion assay (C and G), simulated curves for the Golgi disassembly process according to the successive reaction model were drawn. ○, intact Golgi; △, tubular Golgi; ●, fused Golgi.

Assuming that the kinetics of Golgi tubule formation and Golgi tubule fusion shown in Figure 9 (B, C, F, and G) demonstrated simple linear first-order kinetics, we next estimated the rate constants (k_1, tubule formation rate; k_2, tubule fusion rate) of these elementary processes with the use of generalized least-squares optimization (see MATERIALS AND METHODS). From the optimal fit of each kinetic curve, we obtained the k_1 and k_2 values for nocodazole-untreated (−Noc) and -treated (+Noc) cells (Figure 10). Upon treatment of nocodazole, the rate of Golgi tubulation in semi-intact cells decreased markedly from 0.0842 ± 0.0020 min^{-1} for k_1 (−Noc) to 0.0124 ± 0.0009 min^{-1} for k_1 (+Noc), but the rates of fusion were comparable [k_2 (−Noc), 0.1774 ± 0.0224 min^{-1}; k_2 (+Noc), 0.1971 ± 0.0585 min^{-1}). Based on a series of rate constants and the kinetic model (the successive reaction model), as shown in Figure 10A, we simulated the plots of Golgi disassembly assays in the nocodazole-treated and -untreated semi-intact cells. The simulated curves fit the

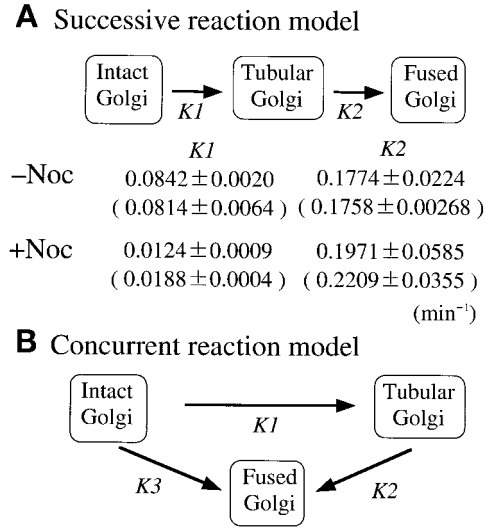

Figure 10. Kinetic model of BFA-induced Golgi disassembly in semi-intact CHO-GT cells. (A) Successive reaction model. In this model, intact Golgi was transformed to tubular Golgi with the rate constant k_1 and then to fused Golgi with the rate constant k_2. Simple linear first-order kinetics through a series of three states of Golgi morphology without a reverse reaction is assumed. Rate constants, obtained from the Golgi tubule formation and Golgi tubule fusion assays, are shown, and those obtained from the Golgi disassembly assay are in parentheses. (B) Concurrent reaction model. In this model, intact Golgi disassembles through two concurrent pathways. One is the successive pathway described in A. The other is a direct pathway in which intact Golgi directly fuses to the ER with the rate constant k_3. Kinetic analysis of the plots from the Golgi disassembly assay (Figure 9, A and B) was preferentially adapted to the successive model.

experimental plots very well (Figure 9, compare A with D and E with H, respectively). The substantial deviations in simulated curves and experimental plots in Figure 9 (A and D) in the period of long incubation (>40 min) seem to represent the loss of activities in our reconstitution system.

Additionally, we obtained the rate constants independently from the plots of the Golgi disassembly assay (Figure 9, A and B) with the use of generalized least-squares optimization to simultaneously fit to the model. Curve fitting was performed, and a series of rate constants was obtained: k_1 (−Noc), 0.0814 ± 0.0064 min^{-1}; k_2 (−Noc), 0.1758 ± 0.0269 min^{-1}; k_1 (+Noc), 0.0188 ± 0.0004 min^{-1}; and k_2 (+Noc), 0.2209 ± 0.0355 min^{-1}. These values were comparable to those from the Golgi tubule formation assay and the Golgi tubule fusion assay.

We also tried to simultaneously fit each kinetic curve from the Golgi disassembly assay (Figure 9, A and B) to an alternative kinetic model, the concurrent reaction model, as shown in Figure 10B. We obtained an optimal fit for each curve when the k_3 (−Noc) and k_3 (+Noc) were almost zero. This indicated little direct fusion between the intact Golgi and the ER membranes and that the fusion was mediated via the Golgi tubules.

We conclude that the slow rate of tubule formation and the lower motility of tubules in nocodazole-treated semi-intact cells may reduce the probabilities of collision and fusion between Golgi and ER membranes.

DISCUSSION

Previous studies on the molecular mechanisms of BFA-induced Golgi disassembly have presumed that the process could be dissected into two elementary parts. First, Golgi tubules are formed. Second, the Golgi tubules fuse to the ER membranes and the fusion results in the rapid relocation of resident Golgi membrane components, protein and lipids, to the ER (Fujiwara *et al.*, 1988; Doms *et al.*, 1989; Sciaky *et al.*, 1997). BFA-induced Golgi tubules are supposed to be key intermediates in the fusion reaction between the Golgi and ER membranes. However, it would be difficult to confirm directly these presumptions and the biochemical requirements for tubule formation, because the tubules usually last only a very short time (5–10 min) and their movements are very dynamic (Sciaky *et al.*, 1997). Neither the biochemical requirements nor the characteristic properties of the fusion process have been confirmed directly.

Our reconstitution system allows one to address these important problems. First, we have succeeded in dissecting the disassembly process into two elementary parts biochemically and morphologically. Second, based on the morphometric analysis, we have established three assays, one for each process: the Golgi disassembly assay, the Golgi tubule formation assay, and the Golgi tubule fusion assay. Using these assays, we have studied the biochemical requirements and kinetics for each process quantitatively and demonstrated several important findings.

Microtubule-dependent Golgi Tubule Formation

To our surprise, the ATP-regenerating system without exogenous cytosol is enough for BFA-induced Golgi tubulation in semi-intact cells (Figures 3 and 4). The high-salt wash (1 M KCl) partially inhibited the ATP-driven tubulation, suggesting that residual factors in semi-intact cells or peripheral membrane proteins, which cycle between the cytosol and the Golgi membranes, are involved in the initial or facilitating step of tubulation. Because microtubule integrity, but not exogenous cytosol, is necessary for this type of tubulation, we call it microtubule-dependent tubulation.

Several investigators have proposed that kinesin-like motor proteins are involved in the formation of tubules (Lippincott-Schwartz *et al.*, 1995; Sciaky *et al.*, 1997). Biochemical analysis with Western blotting showed that almost all of the conventional kinesin (>95%) remained in our semi-intact cells even after extensive washing. Although we failed to inhibit Golgi tubulation with an anti-kinesin mAb, we found that tetracaine, an inhibitor of the in vitro movements of cytoplasmic motors such as kinesin and myosin (Miyamoto *et al.*, 2000), inhibited Golgi tubule formation without affecting the release of β-COP from the Golgi membranes (our unpublished data). The inhibition of tubulation by tetracaine indicates that kinesin-like motor proteins are actually involved in formation.

Rabkinesin-6, another candidate, was identified by a yeast two-hybrid assay with the use of the GTP form of rab6 as bait. The protein contains sequence motifs for ATP binding, which are conserved among kinesin-like proteins, and is involved in the dynamics of the Golgi complex (Echard *et al.*,

1998). However, in the rab-GDI–treated semi-intact cells, Golgi tubule formation was induced by ATP/BFA normally, suggesting that rabkinesin-6 was not involved in tubulation. Recently, new candidates for molecules involved in tubulation were reported by Robertson and Allan (2000). They reconstituted the process of BFA-induced Golgi tubulation with the use of *Xenopus* egg extracts and isolated rat liver Golgi membranes. They showed that H1 antibody, which was raised against bovine kinesin, inhibited tubulation. Surprisingly, key molecules for tubulation detected by H1 antibody were 100- and 130-kDa proteins but not conventional kinesin. These proteins might work in our reconstitution system as well.

Microtubule-independent Golgi Tubule Formation

In nocodazole-treated cells, the Golgi tubules were generated in the presence of NEM cytosol, and they appeared to extend normally (Figure 8A). Hereafter, we call this type of tubulation microtubule-independent tubulation. Compared with the microtubule-dependent Golgi tubules, the motility of microtubule-independent Golgi tubules and the frequency of their bifurcation appeared to be increased, suggesting that the cytosol contains factors that activate the dynamic movements and morphological changes of the tubules. In average lengths and other properties of microtubule-independent Golgi tubules, nocodazole-treated and -untreated semi-intact cells were indistinguishable.

In addition, even in nocodazole-untreated cells, the Golgi tubules did not always extend along with the microtubules. Thus, the microtubule dependence on tubulation is redundant in the presence of cytosol. Our data are partially consistent with previous reports: tubulation is an inherent property of Golgi membranes, because it occurs without the aid of microtubules (Klausner *et al.*, 1992) or BFA treatment (Cluett *et al.*, 1993). Under our assay conditions, nocodazole-treated cells still contain residual microtubules in the periphery of the cells, although NEM cytosol did not induce the substantial reformation of the microtubules. Thus, we cannot completely rule out the possibility that Golgi tubules in nocodazole-treated cells extend along with the residual microtubules through the transient, partial, undetectable interactions between the microtubule and Golgi tubulation.

What kinds of cytosolic factors are involved in microtubule-independent tubulation? One indication comes from the result that GTPγS inhibited tubulation in the presence of cytosol but not in the absence of cytosol. Because the inhibitory effect of cytosol in the presence of GTPγS is not due to the association of COP I coat (Figure 7), the function and the properties of BARS-50 (brefeldin A–ADP-ribosylated substrate) are indicative of the GTPγS-sensitive factor in the cytosol. Weigert *et al.* (1999) demonstrated that BARS-50 is an acyl-CoA transferase catalyzing the acylation of lysophosphatidic acid to phosphatidic acid and that its activity induces the fission of isolated Golgi membranes by altering lipid composition. BFA inhibited the activity of BARS-50, which might result in Golgi tubule formation (Spano *et al.*, 1999). Interestingly, some isoforms of BARS-50 have GTP-binding activity (Di Girolamo *et al.*, 1995), indicating that BARS-50 might be one of the GTPases that inhibit tubulation in our system.

The data described by Jamora *et al.* (1997) are also indicative of the effects of GTPγS on BFA-induced tubulation. They found that GTPγS inhibits illimaquinone-mediated Golgi vesiculation in the presence of cytosol but not in the absence of cytosol. Their findings are very similar to ours with regard to the inhibitory effects of GTPγS in the presence of cytosol. They also demonstrated that illimaquinone-mediated Golgi vesiculation occurs through the activation of trimeric G protein, the free βγ subunit. Such an activation of trimeric G proteins by GTPγS might result in the inhibition of Golgi tubulation as well. However, there is a possibility that the inhibitory effect of GTPγS is not a specific event for BFA-induced Golgi tubulation but a common one in which the morphological changes of the Golgi apparatus occur.

Thus, we suppose that there are two pathways for Golgi tubule formation: one is microtubule-dependent (Figure 4), and the other is microtubule-independent (Figure 8). The former pathway might be induced by the kinesin-like motor protein, depending on microtubule integrity, and the latter might be induced by the exogenous cytosolic factor(s) independent of microtubule integrity and inhibited by GTPγS.

Effects of Microtubule Integrity on Tubule Formation or Fusion

In microtubule-disrupted cells, kinetic studies of tubulation showed that microtubule integrity is likely to affect the initial rate of tubulation but not the fusion of the tubules and the ER (Figures 9, B and F, and 10). Indeed, the rate constant of Golgi tubule formation in the nocodazole-untreated cells is approximately fourfold to sixfold that in nocodazole-treated cells (Figure 10). In our system, the efficiency of Golgi tubulation and the lengths of the tubules in the disrupted cells were similar to those in nocodazole-untreated cells. These results suggest that the microtubule itself is not necessary for fusion but rather serves only to increase the probability of collision between Golgi tubules and the ER membrane networks throughout the cytoplasm.

NSF-dependent Fusion of the Tubules and the ER Membranes

Using our Golgi tubule fusion assay, we found that fusion was mediated mainly by BFA-induced Golgi tubules (Figures 1, 3, and 9). The rate constants of Golgi tubule fusion obtained from the kinetic analysis supported the idea that fusion is mediated mainly via Golgi tubules (the successive reaction model is preferable to the concurrent model in Figure 10) and is independent of microtubule disruption by nocodazole (Figures 9 and 10). In addition, fusion was NEM-sensitive, and the addition of recombinant NSF molecules rescued the fusion inactivity of NEM cytosol (Figure 6B). In contrast, the addition of inactive mutant NSF (K266Q) did not. Together, our results are the first to show that NSF is involved directly in the fusion of the Golgi tubules and the ER membranes.

COP I in Golgi Tubule Formation and Fusion

Scheel *et al.* (1997) demonstrated that one of the antibodies against β-COP interfered with the BFA-induced relocation of resident Golgi membrane proteins to the ER. These findings support the result reported by Donaldson *et al.* (1990, 1991) that GTPγS inhibited the relocation by blocking the dissociation of a 110-kDa protein (β-COP) from the BFA-

treated Golgi complex and suggest that coat proteins inhibit not only Golgi tubulation but also fusion between the Golgi tubules and the ER membranes.

Using our Golgi tubule fusion assay, we confirmed that COP I coat inhibited Golgi tubule fusion to the ER membranes. Our results might also be direct evidence that a coat protein such as β-COP blocks the nonspecific fusion between Golgi tubules and ER membranes by covering the fusion machinery. In addition, our Golgi tubule formation assay demonstrated that GTPγS in the presence of cytosol certainly inhibited tubulation (Figure 7). Thus, our results could be considered consistent with the findings they reported. However, we found that β-COP–depleted rat cytosol also inhibited tubulation in the presence of GTPγS (Figure 7). It was recently suggested that calmodulin antagonists inhibit BFA-induced Golgi tubule formation without affecting the rapid release of COP I (Figueiredo *et al.*, 1998). This finding, together with our results, suggested that BFA-induced Golgi tubule formation is independent of the dissociation of COP I oligomers from the Golgi membranes but is dependent on the GTPγS-sensitive cytosolic factors such as BARS-50 and the free βγ subunit of heterotrimeric G protein described above.

Our dissected reconstitution assays for BFA-induced Golgi disassembly, which are based on the semi-intact cell system coupled with GFP-tagged organelle techniques (Kano *et al.*, 2000), have provided a useful tool with which to study the biochemical requirements of each process and the kinetic analysis of each reaction.

ACKNOWLEDGMENTS

We thank Dr. Mikio Furuse (Kyoto University) for providing the mouse liver cDNA library and for helpful discussions. We also thank Dr. Masao Sakaguchi (Kyushu University) for providing rat cytosol. This work was supported by a Grant-in-Aid for Scientific Research on Priority Areas (B) from the Ministry of Education, Science, Sports and Culture of Japan (M.M.) and by a Research Fellowship of the Japan Society for the Promotion of Science for Young Scientists (F.K.).

REFERENCES

Barak, L.S., Yocum, R.R., Nothnagel, E.A., and Webb, W.W. (1980). Fluorescence staining of the actin cytoskeleton with 7-nitrobenz-2-oxa-1,3-dizole-phallacidin. Proc. Natl. Acad. Sci. USA *77*, 980–984.

Bhakdi, S., Roth, M., Sziegoleit, A., and Tranum-Jensen, J. (1984). Isolation and identification of two hemolytic forms of streptolysin-O. Infect. Immun. *46*, 394–400.

Cluett, E.B., Banta, W.M., and Brown, W.J. (1993). Tubulation of Golgi membranes in vivo and in vitro in the absence of brefeldin A. J. Cell Biol. *120*, 15–24.

Cole, N.B., Sciaky, N., Marotta, A., Song, J., and Lippincott-Schwartz, J. (1996a). Golgi dispersal during microtubule disruption: regeneration of Golgi stacks of peripheral endoplasmic reticulum exit sites. Mol. Biol. Cell *7*, 631–650.

Cole, N.B., Smith, C.L., Sciaky, N., Terasaki, M., Edidin, M., and Lippincott-Schwartz, J. (1996b). Diffusional mobility of Golgi proteins in membranes of living cells. Science *273*, 797–801.

Di Girolamo, M., Silletta, M.G., De Matteis, M.A., Braca, A., Colanzi, A., Pawlak, D., Rasenick, M.M., Luini, A., and Corda, D. (1995). Evidence that the 50-kDa substrate of brefeldin A-dependent ADP-ribosylation binds GTP and is modulated by the G-protein βγ subunit complex. Proc. Natl. Acad. Sci. USA *92*, 7065–7069.

Doms, R.W., Russ, G., and Yewdell, J.W. (1989). Brefeldin A redistributes resident and itinerant Golgi proteins to the endoplasmic reticulum. J. Cell Biol. *109*, 61–72.

Donaldson, J., Lippincott-Schwartz, J., and Klausner, R.D. (1991). Guanine nucleotides modulate the effects of brefeldin A in semipermeable cells: regulation of the association of 110-kD peripheral membrane proteins with the Golgi apparatus. J. Cell Biol. *112*, 579–588.

Donaldson, J.G., Lippincott-Schwartz, J., Bloom, G.S., Kreis, T.E., and Klausner, R.D. (1990). Dissociation of a 110-kD peripheral membrane protein from the Golgi apparatus is an early event in brefeldin A action. J. Cell Biol. *111*, 2295–2306.

Echard, A., Jollivet, F., Martinez, O., Lacapere, J.J., Rousselet, A., Janoueix-Lerosey, I., and Goud, B. (1998). Interaction of a Golgi-associated kinesin-like protein with Rab6. Science *279*, 580–585.

Figueiredo, P.D., and Brown, W.J. (1995). A role for calmodulin in organelle membrane tubulation. Mol. Biol. Cell *6*, 871–887.

Figueiredo, P.D., Drecktrah, D., Katzenellenbogen, J.A., Strang, M., and Brown, W.J. (1998). Evidence that phospholipase A2 activity is required for the Golgi complex and *trans* Golgi network membrane tubulation. Proc. Natl. Acad. Sci. USA *95*, 8642–8647.

Fujiwara, T., Oda, K., Yokota, S., Takatsuki, A., and Ikehara, Y. (1988). Brefeldin A causes disassembly of the Golgi complex and accumulation of secretory proteins in the endoplasmic reticulum. J. Biol. Chem. *263*, 18545–18552.

Fukunaga, T., Furuno, A., Hatsuzawa, K., Tani, K., Ymamoto, A., and Tagaya, M. (1998). NSF is required for the brefeldin A-promoted disassembly of the Golgi apparatus. FEBS Lett. *18*, 237–240.

Hirschberg, K., Miller, C.M., Ellenberg, J., Presley, J.F., Siggia, E.D., Phair, R.D., and Lippincott-Schwartz, J. (1998). Kinetic analysis of secretory protein traffic and characterization of Golgi to plasma membrane transport intermediates in living cells. J. Cell Biol. *143*, 1485–1503.

Jamora, C., Takizawa, P.A., Zaarour, R.F., Denesvre, C., Faulkner, D.J., and Malhotra, V. (1997). Regulation of Golgi structure through heterotrimeric G proteins. Cell *91*, 617–626.

Kano, F., Takenaka, K., Yamamoto, A., Nagayama, K., Nishida, E., and Murata, M. (2000). MEK and Cdc2 kinase are sequentially required for Golgi disassembly in MDCK cells by the mitotic *Xenopus* extracts. J. Cell Biol. *149*, 357–368.

Klausner, R.D., Donaldson, J.G., and Lippincott-Schwartz, J. (1992). Brefeldin A: insights into the control of membrane traffic and organelle structure. J. Cell Biol. *116*, 1071–1080.

Ladinsky, M.S., Kremer, J.R., Furcinitti, P.S., McIntosh, J.R., and Howell, K.E. (1994). HVEM tomography of the trans-Golgi network: structural insights and identification of a lace-like vesicle coat. J. Cell Biol. *127*, 29–38.

Lippincott-Schwartz, J. (1993). Bidirectional membrane traffic between the endoplasmic reticulum and Golgi apparatus. Trends Cell Biol. *3*, 81–88.

Lippincott-Schwartz, J., Cole, N.B., Morotta, A., Conrad, P.A., and Bloom, G.S. (1995). Kinesin is the motor for microtubule-mediated Golgi-to-ER membrane traffic. J. Cell Biol. *128*, 293–306.

Lippincott-Schwartz, J., Yuan, L.C., Bonifacino, J.S., and Klausner, R.D. (1989). Rapid redistribution of Golgi proteins into the ER in cells treated with brefeldin A: evidence for membrane cycling from Golgi to ER. Cell *56*, 801–813.

Miyamoto, Y., Muto, E., Mahimo, T., Iwane, A.H., Yoshiya, I., and Yanagida, T. (2000). Direct inhibition of microtubule-based kinesin motility by local anesthetics. Biophys. J. *78*, 940–949.

Orci, L., Tagaya, M., Amherdt, M., Perrelet, A., Donaldson, J.G., Lippincott-Schwartz, J., Klausner, R.D., and Rothman. J.E. (1991). Brefeldin A, a drug that blocks secretion, prevents the assembly of non-clathrin-coated buds on Golgi cisternae. Cell *64*, 1183–1195.

Robertson, A.M., and Allan, V.J. (2000). Brefeldin A–dependent membrane tubule formation reconstituted in vitro is driven by a cell cycle–regulated microtubule motor. Mol. Biol. Cell *11*, 941–955.

Pimplikar, S.W., Ikonen, E., and Simons, K. (1994). Basolateral protein transport in streptolysin O-permeabilized MDCK cells. J. Cell Biol. *125*, 1025–1035.

Sakaguchi, M., Hachiya, N., Mihara, K., and Omura, T. (1992). Mitochondrial porin can be translocated across both endoplasmic reticulum and mitochondrial membranes. J. Biochem. *112*, 243–248.

Scheel, J., Pepperkok, R., Lowe, M., Griffiths, G., and Kreis, T.E. (1997). Dissociation of coatomer from membrane is required for brefeldin A-induced transfer of Golgi enzymes to the endoplasmic reticulum. J. Cell Biol. *137*, 319–333.

Schnaar, R.L., Weigel, P.H., Kuhlenschmidt, M.S., Lee, Y.C., and Roseman, S. (1978). Adhesion of chicken hepatocytes to polyacrylamide gels derivatized with N-acetylglucosamine. J. Biol. Chem. *253*, 7940–7951.

Sciaky, N., Presley, J., Smith, C., Zaal, K.J.M., Cole, N., Moreira, J.E., Terasaki, M., Siggia, E., and Lippincott-Schwartz, J. (1997). Golgi tubule traffic and the effects of brefeldin A visualized in living cells. J. Cell Biol. *139*, 1137–1155.

Shima, D.T., Haldar, K., Pepperkok, R., Watson, R., and Warren, G. (1997). Partitioning of the Golgi apparatus during mitosis in living HeLa cells. J. Cell Biol. *137*, 1211–1228.

Spano, S., *et al.* (1999). Molecular cloning and functional characterization of brefeldin A-ADP-ribosylated substrate: a novel protein involved in the maintenance of the Golgi structure. J. Biol. Chem. *274*, 17705–17710.

Sumida, M., Hong, R.M., and Tagaya, M. (1994). Role of two nucleotide-binding regions in an N-ethylmaleimide-sensitive factor involved in vesicle-mediated protein transport. J. Biol. Chem. *269*, 20636–20641.

Ullrich, O., Horiuchi, H., Alexandrov, K., and Zerial, M. (1995). Use of Rab-GDP dissociation inhibitor for solubilization and delivery of Rab proteins to biological membranes in streptolysin O-permeabilized cells. Methods Enzymol. *257*, 243–253.

Weidman, P., Roth, R., and Heuser, J. (1993). Golgi membrane dynamics imaged by freeze-etch electron microscopy: views of different membrane coatings involved in tubulation versus vesiculation. Cell *75*, 123–133.

Weigert, R., *et al.* (1999). CtBP/BARS induces fission of Golgi membranes by acylating lysophosphatidic acid. Nature *402*, 429–433.